EARTH SURFACE PROCESSES AND LANDFORMS
Earth Surf. Process. Landforms (2012)

Published online in Wiley Online Library
(wileyonlinelibrary.com) DOI: 10.1002/esp.3299

Properties of natural supraglacial debris in relation to modelling sub-debris ice ablation

Lindsey Nicholson[1]* and Douglas I. Benn[2,3]
[1] Centre for Climate and Cryosphere, Institute for Meteorology and Geophysics, University of Innsbruck, Innsbruck, Austria
[2] Department of Arctic Geology, University Centre in Svalbard, Longyearbyen, Norway
[3] School of Geography and Geosciences, University of St Andrews, St Andrews, Fife, UK

Received 13 March 2012; Revised 15 June 2012; Accepted 28 June 2012

*Correspondence to: Lindsey Nicholson, Centre for Climate and Cryosphere, Institute for Meteorology and Gephysics, University of Innsbruck, Innsbruck, Austria.
E-mail: lindsey.nicholson@uibk.ac.at

ESPL
Earth Surface Processes and Landforms

ABSTRACT: As debris-covered glaciers become a more prominent feature of a shrinking mountain cryosphere, there is increasing need to successfully model the surface energy and mass balance of debris-covered glaciers, yet measurements of the processes operating in natural supraglacial debris covers are sparse. We report measurements of vertical temperature profiles in debris on the Ngozumpa glacier in Nepal, that show: (i) conductive processes dominate during the ablation season in matrix-supported diamict; (ii) ventilation may be possible in coarse surface layers; (iii) phase changes associated with seasonal change have a marked effect on the effective thermal diffusivity of the debris. Effective thermal conductivity determined from vertical temperature profiles in the debris is generally ~30% higher in summer than in winter, but values depend on the volume and phase of water in the debris. Surface albedo can vary widely over small spatial scales, as does the debris thickness. Measurements indicate that debris thickness is best represented as a probability density function with the peak debris thickness increasing down-glacier. The findings from Ngozumpa glacier indicate that the probability distribution of debris thickness changes from positively skewed in the upper glacier towards a more normal distribution nearer the terminus. Although many of these effects remain to be quantified, our observations highlight aspects of spatial and temporal variability in supraglacial debris that may require consideration in annual or multi-annual distributed modelling of debris-covered glacier surface energy and mass balance.

KEYWORDS: supraglacial debris; thermal conductivity; ablation modelling; debris-covered glaciers

Introduction

Debris-covered glaciers are a prominent feature of many high relief mountain ranges such as the Himalaya, and there is increasing need to model their behaviour in sufficient detail to improve management of hydrological resources. Supraglacial debris cover on glaciers influences the ablation regime of the underlying ice by altering the surface energy balance and imposing a barrier between the atmosphere and the ice. Variations in surface temperature, primarily driven by diurnal and seasonal cycles, propagate through the debris profile with the same period, but decreasing amplitude and increasing lag, dependent on depth and the efficiency with which the debris can transfer heat (e.g. Farouki, 1981; Williams and Smith, 1989). The damping depth of a surface temperature fluctuation is proportional to the period of oscillation, so longer period oscillations, such as a seasonal variation, will penetrate deeper into the profile than diurnal temperature oscillations. Beneath a thin debris cover additional energy from the enhanced absorption of short wave radiation resulting from the lower albedo of the debris cover is transmitted efficiently to the ice beneath and melt rate is accelerated compared to that of bare ice. Debris thicker than a few centimetres in thickness does not reach thermal equilibrium with diurnal oscillations of surface temperature (Reznichenko *et al.*, 2010) and energy consumed in heating the debris cover during the daytime is returned to the atmosphere at night, rather than being transmitted efficiently to the ice below. Hence, beyond a critical thickness, which is dependent on the optical and thermal properties of the debris as well as the meteorological conditions, melt is less than that of bare ice surfaces (Østrem, 1959; Loomis, 1970; Fujii, 1977; Nakawo and Young, 1982; Mattson *et al.*, 1993; Nicholson and Benn, 2006). Extensive, thick debris cover on glacier surfaces generally retards ice ablation, and compared with clean ice glaciers, debris-covered glaciers extend to lower altitudes, and may persist through warmer climatic periods. Thus, debris-covered glaciers have a different extent to clean-ice glaciers under the same climate, and will respond differently to the same climatic forcing (Jansson and Fredin, 2002).

Very thick debris covers (> 1 m) are typical in the lower portions of Himalayan debris-covered glaciers, and in these cases it has been shown that ablation by backwasting of near-vertical ice cliffs plays a significant role in ice ablation on the lower tongues despite the fact that exposed ice comprises only a small percentage of the surface area (Sakai *et al.*, 2000). At the upper end of the debris-covered ice area the debris is

thinner, surface relief is more muted, and there are often no ice cliffs or ponded water. Maximum rates of sub-debris ablation are predicted in this zone of thinner, emerging debris cover and determining ablation rate here is critical in determining how surface lowering interplays with ice flux to influence the development of the glacier long profile through time (Nicholson, 2005; Benn and Evans, 2010; Benn *et al.*, 2012).

Due to the difficulties of obtaining and extrapolating direct ablation measurements over debris-covered glaciers, mathematical modelling of melt rate from meteorological variables is preferable (e.g. Nakawo and Young, 1982; Nicholson and Benn, 2006; Reid and Brock, 2010). Within porous material, such as supraglacial debris, energy transfer can occur through conduction, radiation, convection, advection (via a fluid) and phase changes (Farouki, 1981; Humlum, 1997; Putkonen, 1998), but for simplicity, most sub-debris ice ablation models treat all energy transfer as if it were a conductive energy flux [Q_c (in $\mathrm{W\,m^{-2}}$)] governed by the effective conductivity of the debris layer [k_e (in $\mathrm{W\,m^{-1}\,K^{-1}}$)] and the gradient of temperature [T_d (in kelvins)] within the debris. Assuming lateral temperature gradients are small compared to vertical temperature gradients, the one-dimensional energy flux in the vertical [z (in metres)] direction is:

$$Q_c = -k_e \frac{\partial T_d}{\partial z} \tag{1}$$

When the ice temperature is below 0°C any positive conductive heat flux through the debris to the ice interface will be conducted into the ice body. When the ice reaches 0°C, the melt rate [M (in $\mathrm{m\,s^{-1}}$)] expressed as a lowering rate can be computed from the conductive energy flux at the debris–ice interface, the latent heat of fusion [L_f (in $\mathrm{J\,kg^{-1}}$)] and the density of ice [ρ_i (in $\mathrm{kg\,m^{-3}}$)]:

$$M = \frac{Q_c}{L_f \rho_i} \tag{2}$$

If the debris properties are known, and meteorological data are available, the debris surface temperature (T_s) can be determined from the surface energy balance over a given timestep (e.g. Nakawo and Young, 1982; Han *et al.*, 2006; Nicholson and Benn, 2006; Reid and Brock, 2010) and the sub-debris and en-glacial temperature field and resultant energy flux for melt can be computed.

The use of automatic weather stations to estimate surface energy balance is well developed, but determining debris properties for model input remains a challenge. It is known that the composition, thickness distribution and moisture content of the debris cover vary in space and time. However, the scarcity of published data on the properties of supraglacial debris and the uncertainty of the significance of processes operating within it, hamper the development of physical models of sub-debris ablation.

For spatially distributed modelling of mass balance of debris-covered glaciers it is desirable to understand to what extent the system can be simplified whilst retaining the capability to produce realistic mass change distributions and melt-water production rates. The model system outlined earlier assumes that it is reasonable to model all energy flux within the debris as conductive. It also requires knowledge of the effective thermal conductivity of the debris, the thickness of the supraglacial debris cover and its surface albedo, and how these variables vary in space and time.

Determining the validity of treating all energy flux as conductive transfer, and investigating the effective thermal conductivity of supraglacial debris requires monitoring of its thermal regime. Early experiments on the effect of debris cover on ablation rate used artificially applied sediments with known thermal and structural properties (e.g. Drewry, 1972; Nakawo and Young, 1981), and only a few short-term studies have been made in supraglacial debris (e.g. Conway and Rasmussen, 2000). However, thermal monitoring of ground, blockfield and rock glacier conditions is relatively common in permafrost studies (Vondermuhll and Haeberli, 1990; Hinkel, 1997; Humlum, 1997; Harris and Pedersen, 1998; Putkonen, 1998). These studies show that conduction of heat, phase changes of water and infiltration of liquid water all contribute to the energy flux (Equation (1)) and explanation of observed temperature records (Putkonen, 1998). Phase changes dominate because the thermal conductivity of ice is four times that of water, while its mass heat capacity is half that of water, and it releases significant amounts of latent heat (Conway and Rasmussen, 2000). Laboratory experiments have shown that permeability can have a marked effect on heat flux through a debris layer by altering infiltration and interstitial refreezing of water from the surface (Reznichenko *et al.*, 2010).

Here we present data on the thermal regime of supraglacial debris on a Himalayan glacier measured over an annual cycle, which allows a first assessment of how well simplified representations of the thermal properties of supraglacial debris layer reflect reality, and how the simplifications may impact models of sub-debris ablation. Three sites with contrasting grain size and stratigraphy are compared over short-time scales and then debris temperatures in typical supraglacial diamict are observed for an 11-month period. These measurements capture the thermal properties of the debris and processes operating within it over the range of debris types found on the glacier and through time. We also present a brief analysis of field observations of spatial and temporal variability in debris surface albedo and thickness at the same glacier. These data provide information for incorporating the impact of supraglacial debris cover in distributed glacier mass balance modelling over multi-annual timescales.

Field Site and Data Description

The study site is the Ngozumpa glacier in the Khumbu Himal region of the eastern Nepalese Himalaya (27°56′00″N; 86°42′45″E). The lower 15 km of the 18 km long glacier is slow-moving or stagnant (Quincey *et al.*, 2009) and has a mature debris cover and numerous supraglacial ponds (Benn *et al.*, 2001). Local geology is predominantly sillimanite grade gneiss, and more resistant Makalu leucogranite (Kostlin and Molyneux, 1992). Observations indicate that debris thickness increases down-glacier and can exceed 1·5 m near the terminus (Nicholson, 2005). The debris surface is typically coarse, clast-supported material beneath which the debris is unsorted matrix-supported diamict. The thickness of the coarse surface layer varies considerably, and the clasts within it vary from the sub-centimetre to decimetre scale (Figure 1; Nicholson, 2005). The diamictic nature of much supraglacial debris suggests that the debris may have multiple sources and transport pathways and in addition to melt-out of en-glacial debris, fine rock flour from lateral moraines is redistributed onto the glacier surface (Singh *et al.*, 2000; Hands, 2004). Stratified sediments occur locally in the debris layer, recording gravitational and fluvial reworking and lacustrine deposition typical of mature debris-covered glacier surfaces (Figure 1d; Benn and Owen, 2002). Differential melt has resulted in significant surface relief on the debris covered portion of the glacier with hummocky terrain ranging from 10 to 50 m in height. The ice temperature of the Ngozumpa has not been measured

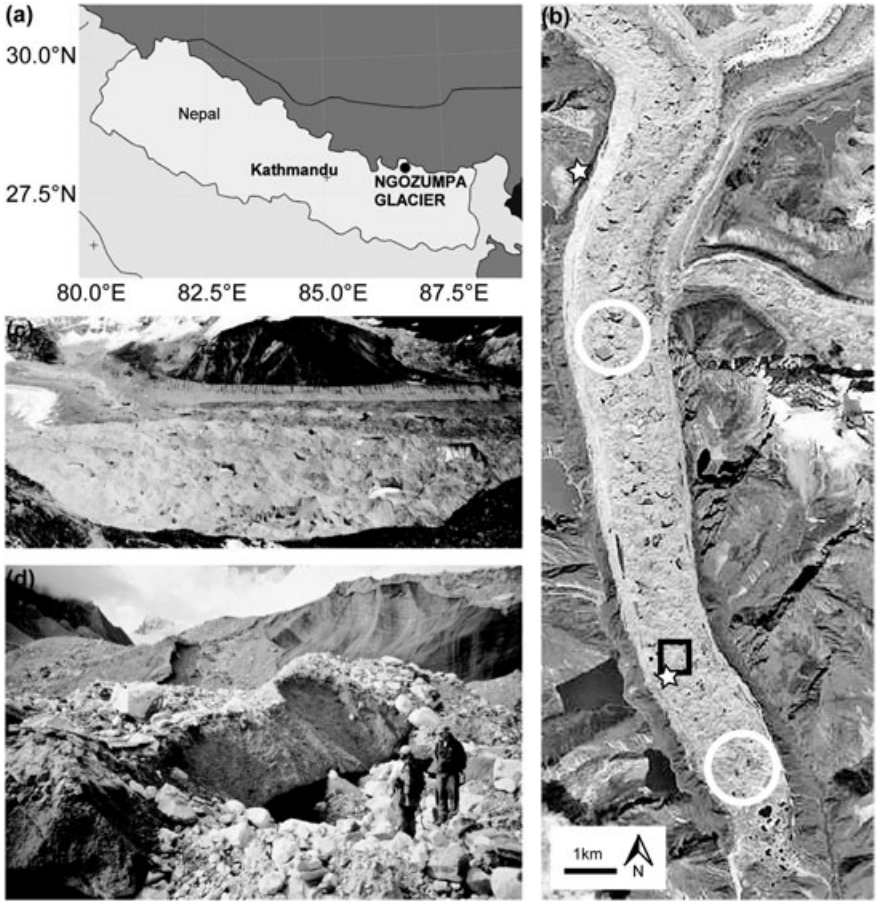

Figure 1. (a) Location of Ngozumpa glacier in the eastern Himalaya of Nepal; (b) SPOT image (January 2000) of the debris-covered portion of the Ngozumpa glacier showing the site of the debris temperature measurements and automatic weather station (within black box), the locations of debris thicknesses surveys (within white circles), and approximate positions from which photographs (c) and (d) were taken (stars); (c) overview of the debris covered glacier surface; (d) detail of the surface conditions showing a variety of debris reworking processes and the variety of debris particle size distribution.

beneath the debris cover, but temperature measurements from within en-glacial caves within the ablation zone show ice to be about 0°C, with the exception of a cold winter surface layer in the vicinity of cave entrances.

Vertical temperature profiles in naturally occurring supraglacial debris were measured using an array of six thermistors (Table I). The measurements sites were all ~3 km from the glacier terminus at an elevation of ~4800 m (Figure 1b). Thermistors were installed by excavating a pit, emplacing the thermistor probes in the sidewall of the pit, and replacing the debris as best as possible in its original stratigraphic sequence. The maximum error on the vertical position of the sensor is estimated to be 0·01 m. Temperatures were recorded every 30 minutes and temperature timeseries at all thermistor levels stabilized within three days of installation. Consequently analyses were carried out using data from day 4 and onwards at each site. Concurrent meteorological measurements (Table I) facilitate interpretation of the debris temperatures, although the record is incomplete due to power failures during cold nocturnal conditions when the data logger failed to record

Table I. Details of the instrumentation used in the study.

Parameter	Height (m)				Sensor	Accuracy
Air temperature	1·5				Campbell 50Y	± 0·35°C
Relative humidity	1·5				Campbell 50Y	± 2–6%
Incoming shortwave radiation	at surface				Kipp & Zonen CM21	± 2% (day total)
Incoming longwave radiation	at surface				Kipp & Zonen CG1	± 10% (day total)
Wind speed	1·5				Campbell A100R	± 0·1 m s^{-1} < 10 m s^{-1}
	Depth of sensor (m)					
Debris temperature	(i)	(ii)	(iii)	(iv)	Gemini PG5001	± 0·3 at 0°C
	0·00	0·00	0·20	0·00		
	0·14	0·15	0·30	0·22		
	0·24	0·30	0·50	0·33		
	0·35	0·45	0·65	0·45		
	0·42	0·60	0·75	0·65		
	0·60	0·70	1·00	0·77		

Note: Meteorological instruments were used in conjunction with a Campbell CR510 datalogger and the thermistors within the debris cover were connected to individual Gemini TinyTag data loggers.

and at the end of the record when the 12 volt battery was becoming exhausted. Data gaps in January, February and March were 15, 24 and 18%, respectively. Only days with no missing data were used to compute daily mean values so the record does not extend beyond 8 September 2002 after which all days contained some missing data as the battery power was depleted.

Profiles of debris temperatures were measured for 10 days in naturally occurring debris sections consisting of (i) typical supraglacial diamicton, (ii) silt within a former supraglacial lake bed, and (iii) cobbles grading into coarse diamicton at 0·5 m to evaluate the impact of debris cover composition on the measured temperatures. Subsequently, the thermistors were re-installed in (iv) a second location with typical supraglacial diamicton at a stable site from 13 November 2001 to 12 October 2002. The thermistor profiles only reached the glacier ice surface at site (i) and at the other sites the thickness of the debris is not known because excavations to glacier ice were not carried out due to limitations of time and manpower. The chosen sites were on open, level terrain and were not affected by any visible gravitational or fluvial reworking over the course of the experiment and at the end of the experiments thermistor locations were measured to be within 1 cm of their initial measured position.

The matrix-supported diamict that is typical of the supraglacial debris consists of clasts of predominantly schist and leucogranite from gravel to boulder size within a light grey matrix. The surface of the debris cover is highly variable with diamict being overlain with anything from large boulders (> 2 m), cobbles, pebbles or even fine silts. The thickness of these surface layers varies from a few centimetres to more than a metre. The character of the surface layer results from fall sorting, fluvial action and collapse of the ice beneath.

The debris cover at sites (i) and (iv) consisted of the characteristic unsorted matrix-supported diamict throughout the depth of the sampled profile. In the sections measured here maximum clast size was ~10 cm and particle size analysis of the matrix material using a Coulter LS230 identified a bimodal particle size distribution of fine and coarse sands. At site (ii) the sampled depth of the debris cover was a thick layer of fine laminated lacustrine silt in a former lake basin. The silt was grey at depth while the top 2 cm were desiccated and had a very bright surface. At site (iii) the upper 0·5 m consisted of clast-supported coarse cobbles, and below 0·5 m the thermistors were in matrix-supported diamict with a coarser matrix than described for sites (i) and (iv). Maximum clast size within the top 0·5 m was ~20 cm, with most cobbles being 10–15 cm in maximum dimension. The clasts were a mix of bright leucogranite and darker schist. More detailed observations of the specific lithology of the sites were not made, but mineralogical analysis of samples from the same study site indicate composition is predominantly quartz, calcium albite feldspar and biotite mica (Casey *et al.*, 2012).

The linearity of temperature profiles was assessed by computing Pearson's correlation for all six thermistors and using the r^2 value as an index of linearity although the values are not significant in a statistical sense, and this method does not account for errors in the vertical position of the sensor. These index values were only considered valid when the standard deviation across the six thermistors was > 0·8°C.

Effective thermal diffusivity [κ_e (in $m^2 s^{-1}$)] of the debris was computed at the points of the four central thermistors as the ratio of the first derivative of hourly temperature with time [t (in seconds)] against the second derivative of hourly temperature with depth for unevenly spaced points (Williams and Smith, 1989; Conway and Rasmussen, 2000):

$$\frac{\partial T_d}{\partial t} = \kappa_e \frac{\partial^2 T_d}{\partial z^2} \tag{3}$$

The gradient of the linear regression provides an estimate of the average diffusivity for that depth and the scatter around the regression indicates non-conductive processes. For example, instances where the change in temperature with time is low but the change in rate of temperature change with depth is large indicate phase changes in the debris layer (Williams and Smith, 1989; Conway and Rasmussen, 2000). Conway and Rasmussen (2000) showed that the error associated with κ_e computed by this method is not affected by the sensor error or the positional error as long as both of these are constant in time, which is assumed to be the case. Although other methods to determine κ_e exist, this one is considered most applicable in cases where substantial phase changes are suspected (Williams and Smith, 1989)

Effective thermal conductivity [k_e (in $W m^{-1} k^{-1}$)] was calculated from κ_e by

$$k_e = \kappa_e \rho_d c_d, \tag{4}$$

where ρ_d and c_d are the density and specific heat capacity of the debris respectively. Volumetric heat capacity of the debris was calculated from standard values of density (2700 kg m^{-3}) and specific heat capacity (750 J kg^{-1} K^{-1}) for rocks. The bulk volumetric heat capacity is the mean of that of the debris and the void filler weighted by the porosity, which was determined based on Coulter counter analysis of particle size distribution of the debris matrix to be fine sand, with a sub-component of coarse sand, with a bulk effective porosity of ~0·33. The error on the volumetric heat capacity is estimated to be 10% (Conway and Rasmussen, 2000).

Measurements of surface albedo were made using a Campbell CM3 pyranometer held at a distance of 0·5 m from the surface and allowed to stabilize for 30 to 60 seconds. Fifty spot locations were sampled in an irregular grid at approximately level surfaces over an area of *c.* 1600 m^2 around the site of the thermistor installation. All measurements were made during clear sky conditions and all sampled surfaces were dry, but sampling times varied between 10:00 h and 14:00 h. Samples were made over an area including coarse and fine surface material including some areas with dark organic matter at the surface. The error associated with these hand-held measurements is expected to be large and the data are used here in a descriptive rather than quantitative sense.

Debris thickness was sampled at locations 1 km (n = 94) and 7 km (n = 124) from the glacier terminus (Figure 1b) by measuring the debris thickness exposed above ice cliffs using a laser theodolite and reflector positioned at the upper debris surface. As it is dangerous to access the edge of the ice and debris cliff, the distance and dip to the reflector positioned at the crest of the debris was measured and then the dip to the debris–ice interface vertically below the reflector along the line of sight was measured. Debris thickness was computed from the vertical difference in the two dip readings, assuming that the debris face was vertical. The sources of error associated with this method are (a) the obliquity of view angle and (b) the sub-vertical slope angle of the debris exposures being measured, and these were not quantified. The theodolite was continually moved to maintain a perpendicular view of the ice face being surveyed to minimize errors associated with (a) and, as debris exposures at ice cliffs on the Ngozumpa glacier typically take the form of cliffs, with slope angles significantly greater than the angle of repose the error associated with (b) is acceptable for determining spatial

variability in debris thickness. The survey in the upper glacier was taken from the west lateral moraine so all samples are from west-facing ice cliffs, but in the lower ablation zone the surveys were made from the glacier surface and sampled ice faces of all orientations. The cliff orientation should not affect the debris thickness measurements as care was taken to sample along the full length of the cliff so that thicknesses were measured at all levels of the topography that the cliff line intersected. Debris thicknesses were also sampled at the location of the temperature measurements at 4 km for the terminus, but here the vertical dimension of exposed debris cover sections were surveyed using triangulation and the results are less reliable than those determined with the laser distomat and reflector as the method relies on accurately re-identifying individual targets within the debris, and consequently the data are not presented here.

Debris Temperatures and Temperature Profiles in Debris of Different Grain Size

The gradient of the mean temperature profile over timescales of a few days is expected to be linear if (1) non-conductive processes are not influential, (2) thermal conductivity is constant with depth, and (3) there is no change in heat storage over the time interval of the averaging. Figure 2 shows mean temperature profiles measured over days 4 to 6 at sites (i) to (iii). A snowfall occurred during the measurements in the diamict [site (i)] and, during the latter half of the measurements in the cobbles [site (iii)], the air temperature decreased progressively. To avoid the impact of these factors a sub-set of three days is shown for which meteorological conditions were relatively stable. Inclusion of the other days sampled does not change the overall form of the vertical profiles of mean temperature. At sites (i) and (ii) the uppermost thermistors were measuring surface temperature and were initially covered by a thin layer of fine sediment. However this was rapidly lost and data from these surface thermistors were excluded from the analysis because they were affected by direct solar heating. At site (iii) the uppermost sensor was below the surface and was thus not affected by direct solar radiation. The three sites show a marked difference in the behaviour of the temperature profiles despite being located within a few tens of metres of each other. However, any comparison between sites should be undertaken with caution because measurements were taken on different dates, during the time of autumn transition, and in different depths of debris. Although the dataset for each site is short, the following paragraphs summarize the features of the observed debris temperatures.

During the measurements in diamict [site (i)] air temperature was persistently above 0°C, averaging 2·2°C. The lowest thermistor in the diamict was emplaced at the ice interface where a constant temperature of $-0{\cdot}2 \pm 0{\cdot}3$°C was recorded. Liquid water was found at the ice surface during both excavations, which suggests that melt was occurring over the course of the measurement period. The mean temperature profile is not linear, and the cold departure from a linear mean temperature profile towards the ice interface could result from the ongoing melt acting as a heat sink.

In the silt layer [site (ii)] the mean temperature profile is linear and shows little variation with depth. There is no evidence on non-conductive processes operating within the silt. The low mean air temperature (−2·0°C) that prevailed over the measurement period did not cause inversion of the temperature gradient which remains slightly positive, indicating that solar heating of the debris surface has a strong control on the temperature profile. There is a significant lag in peak temperature between the air temperature and peak debris temperatures indicating that the effective thermal diffusivity of this material under the influence of the small vertical temperature gradient is low.

During the measurements in debris with surface cobbles grading into coarse diamict [site (iii)], the air temperature progressively increased, with a mean of −0·9°C. The three-day and mean temperature gradient is distinctly non-linear. At a depth of 0·2 m, nocturnal temperatures closely match the above-surface air temperature with no time lag. This suggests that voids in the debris layer are well connected with the surface air flow and that nocturnal temperatures within

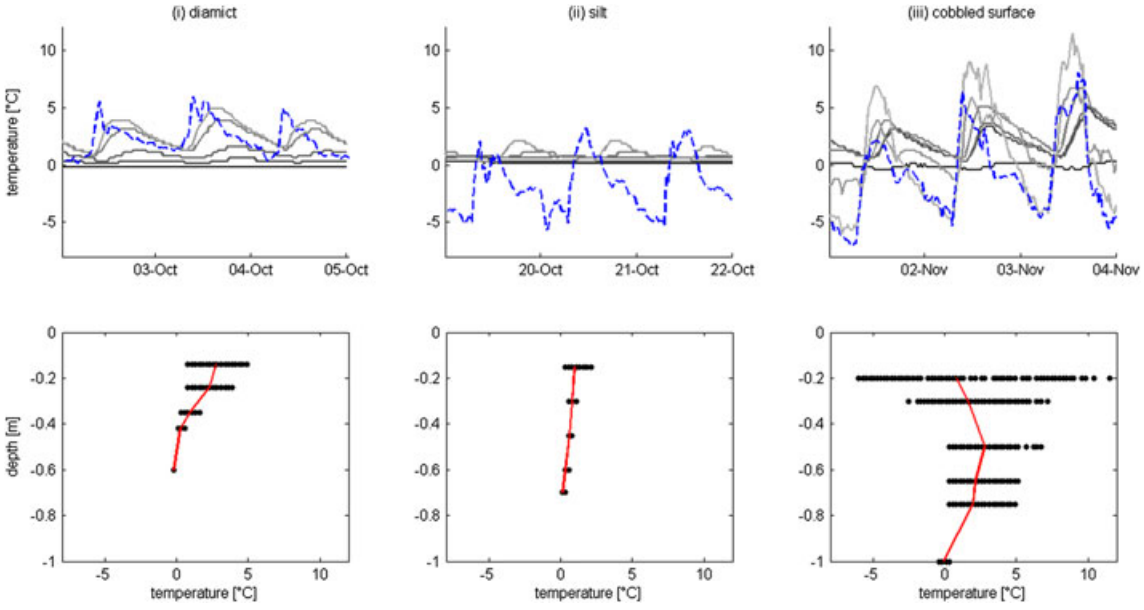

Figure 2. Three-day temperature timeseries and mean temperature profiles in supraglacial (i) diamict, (ii) silt and (iii) cobbles transitioning to matrix-supported diamict at ~0·5 m depth. In the upper panel, air temperature is shown in the dashed line and debris temperatures in shades of grey getting darker with depth. The labelled date refers to the initial midnight of that day. In the lower panel the hourly temperatures recorded at each level are shown as dots and the three day mean temperature profile is shown as a line plot. This figure is available in colour online at wileyonlinelibrary.com/journal/espl

the debris layer rapidly equilibrate to air temperatures by processes presumably including radiative cooling, and buoyant air displacement or ventilation from above. Daytime temperatures at 0·2 m depth exceed the air temperature by several degrees, and this is attributed to radiative heat exchanges within the coarse surface layer where boulder surfaces are heated by direct sunlight. These non-conductive processes cause the mean temperature profile to be persistently inverted above 0·5 m despite the fact that the mean temperature throughout the debris layer increased by 1–2°C in response to the increase of maximum daytime and minimum night-time air temperatures over the measurement period. Mean temperature profiles of each individual day also display the near-surface inversion as shown in Figure 2.

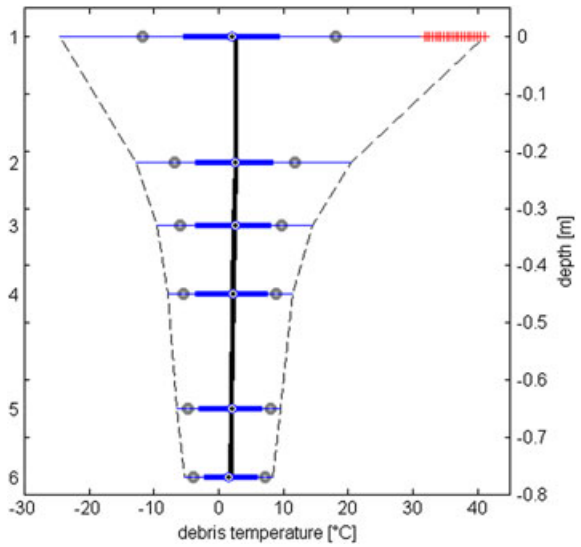

Figure 3. Summary of debris temperatures measured at 30 minute intervals by thermistors 1–6 in diamict at site (iv) from 13 November 2001 to 12 October 2002 inclusive. The solid horizontal bars are the interquartile range, with the median highlighted by a target, and circles show the 10th and 90th percentiles of the measured temperatures. The horizontal lines extend to 1·5 times the interquartile range, and outliers from this are highlighted as crosses (only occur in the upper temperature record). The cone of the minimum and maximum temperatures is shown in dotted lines. This figure is available in colour online at wileyonlinelibrary.com/journal/espl

The bottom temperature of all three profiles is close to 0°C despite the fact that only the profile at site (i) extended to the underlying glacier ice. At site (i) the bottom temperature is constant throughout the experiment while at sites (ii) and (iii) the standard deviation of temperature over the three day period was 0·07 and 0·20°C, respectively.

Debris Temperatures and Temperature Profiles over an 11-month Period

Distribution of measured debris temperatures

The mean temperature profile over the 11 months measured at site (iv) is linear, and has a very slightly positive gradient, with a value of 2·6°C at the surface and 1·8°C at 0·77 m depth (Figure 3). The temperature distribution is asymmetrical with more extreme positive temperatures than extreme negative temperatures in the near surface layer.

Seasonal variability in debris temperature

Diurnal oscillations imposed by surface meteorology do not generally penetrate below 0·5 m at the study site, but seasonal changes penetrate deeper than the lowest thermistor (Figure 4). Assuming that the thermal properties in the upper 0·77 m are representative for the whole debris cover, the temperature cone from Figure 3 can be extrapolated to indicate the maximum depth of influence of the annual temperature wave would be at 1·6 m (Williams and Smith, 1989). This is a crude estimate but would imply that no ablation can be expected beneath debris covers greater than this thickness if the maximum and minimum temperatures sampled over this period are representative of the current climatic conditions.

Positive temperatures are possible near the surface during the daytime in winter (Figure 4a), but the bulk of the debris cover remains below 0°C, and daily mean temperatures are all below 0°C (Figure 5a). The mean temperature profile crosses the 0°C threshold over the course of a month following snowmelt in early March, during which time the daily mean temperatures are quasi-constant throughout the sampled depth. Mean daily surface debris temperature crosses the 0°C threshold only two weeks ahead of the lowest thermistor, and just ahead of daily mean air temperatures (Figure 5a and 5c).

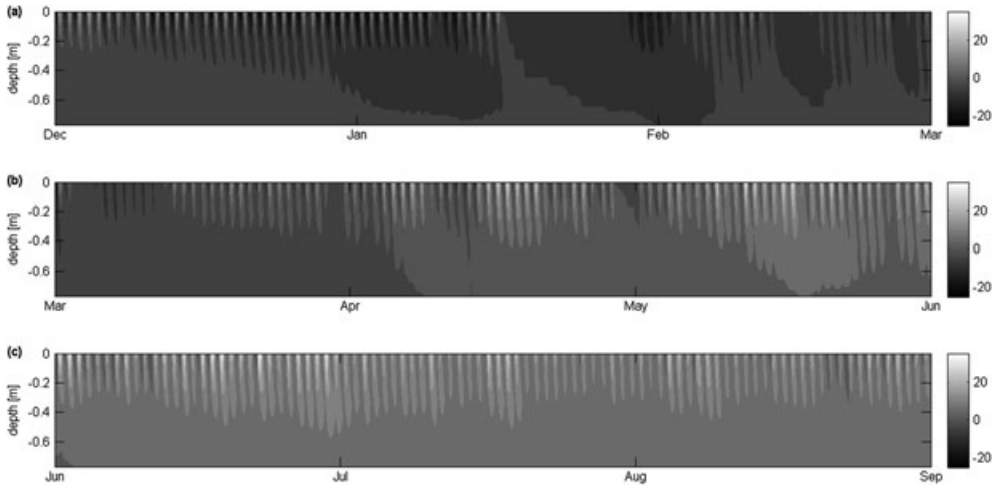

Figure 4. Temperatures at intervals of four hours for the three seasons that are sampled in full (a) winter [December, January, February (DJF)]; (b) spring [March, April, May (MAM)]; (c) summer [June, July, August (JJA)].

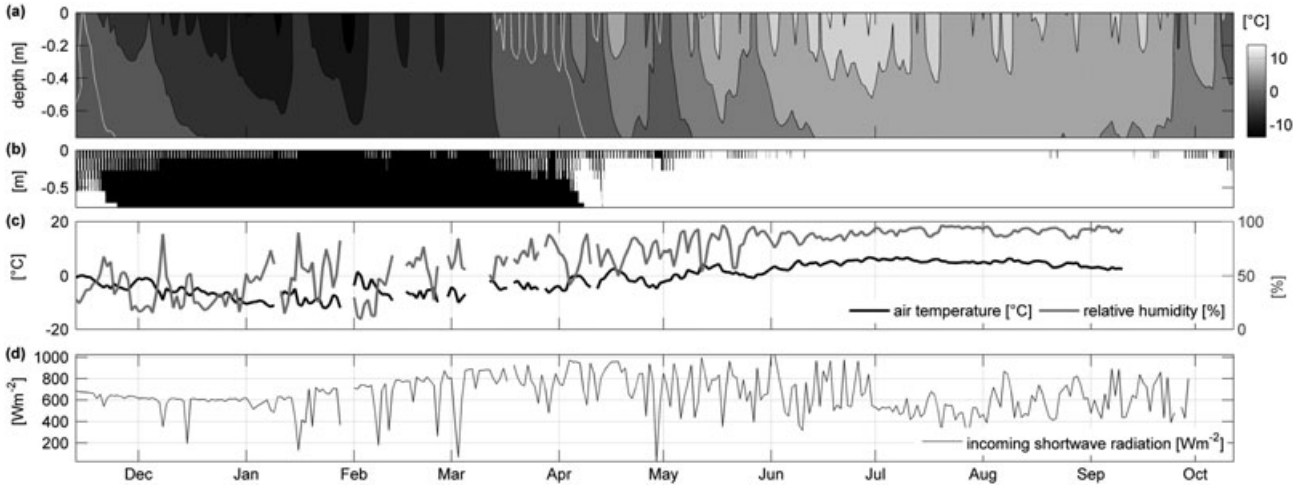

Figure 5. (a) Daily mean debris temperatures (°C) with the daily mean 0°C isotherm shown in white; (b) 30 minute temperatures < 0°C (black) and 0°C (white); (c) mean daily air temperature and relative humidity for days when > 14 of 24 hourly measurements were available; (d) mean incident shortwave radiation between 9:00 h and 15:00 h.

By May, positive daily mean temperatures are clearly established throughout the sampled depth of the debris cover. During the monsoon months of July, August and September (JAS), incoming shortwave radiation is reduced by the development of thick cloud cover at the site, which reduces the occurrence of surface temperatures > 25°C, and causes mean debris temperatures to peak at the end of June, even though air temperatures remain high throughout July and August (Figure 5, Table II).

If there is moisture present in the debris layer, phase changes could be exerting an influence on the thermal regime of the debris cover during seasonal transition periods and in the upper portion of the debris layer throughout much of the winter when the surface is not snow covered (Figure 5b), and previous work suggests ignoring phase changes at the surface can lead to significant errors in modelled sub-debris ablation (Sakai and Fujita, 2004).

Snowfall events of sufficient magnitude to bury the radiometers installed at the debris surface are indicated by extreme minima in the incident shortwave radiation record (Figure 5d). Snow cover, such as occurred in mid-January, immediately prevents the penetration of the diurnal cycle into the debris, which rapidly equilibrates to a uniform temperature (Figures 4a and 5a) and subsequently the debris layer slowly cools at all levels. In the absence of additional concurrent field observations at this site it is difficult to determine details of the impact of snow ablation on the thermal regime of the debris layer, but modelling work suggests that ground temperatures can be expected to be influenced by infiltration of melt-water from overlying snow (Scherler *et al.*, 2010). Anomalously high temperatures at the beginning of February cause a rapid warming of the upper debris layers, and the re-appearance of a diurnal warm wave that rises above zero degrees in Figure 4 indicates that the surface is no longer snow covered.

Vertical temperature gradients

Although instantaneous temperature profiles in debris layers more than a few centimetres thick are non-linear as the surface temperature changes occur at a faster rate than the energy transfer in the debris layer, 24-hour average temperature profiles under stable conditions are often well approximated by a linear gradient (Nicholson, 2005; Nicholson and Benn, 2006). The daily linear gradient with depth in mid-summer ($-10{\cdot}5°C\,m^{-1}$ in June) and mid-winter ($9{\cdot}1°C\,m^{-1}$ in December) are of similar magnitude but opposite sign, indicating heat flux away from the ice in winter. In mid-summer the diurnal temperature cycle penetrates ~0·2 m deeper than in mid-winter. The linear gradient between summer [June, July, August (JJA)] mean mid-day temperature at the upper and lowermost thermistors is $-21{\cdot}4°C\,m^{-1}$, which is double the daily mean gradient over the same season.

Only half of the sampled days have daily mean temperature profiles for which the index of linearity conditions are met (r^2 of linear least squares fit 0·95 and standard deviation of the six thermistors > 0·8) (Figure 6). Days that do not meet these criteria occur mainly during the seasonal transitions (Figure 7), when non-conductive processes are more likely to contribute to the thermal regime (Figure 5b), but mean temperature profiles also fail this linearity test in response to normal variation in meteorological conditions during the summer season.

Although only the upper 0·77 m of debris were sampled, extrapolation of the regression line to its 0°C intercept (Figure 6c) illustrates the pattern of progression the freezing front might take at greater depths in the debris. Extrapolation of linear mean temperature has been used as an indicator of likely minimum debris thickness (Conway and Rasmussen, 2000), but the data here suggest that debris thickness determined this way will be strongly variable in time, and unreliable if the debris extends far beyond the lowest thermistor. At this site the 0°C intercept of

Table II. Maximum and mean changes in day-to-day mean debris temperatures through the profile.

Depth (m)	0·00	−0·22	−0·33	−0·45	−0·65	−0·77
Maximum positive change	4·0 (8·4)	3·4 (4·6)	2·4 (2·8)	1·3 (1·6)	0·7 (0·8)	0·5 (0·8)
Maximum negative change	−3·8 (−6·6)	−3·1 (−4·4)	−3·6 (−3·6)	−2·5 (−2·5)	−1·0 (−1·0)	−0·7 (−0·8)

Note: Values are given for the JJA melt season and in brackets for the whole time series.

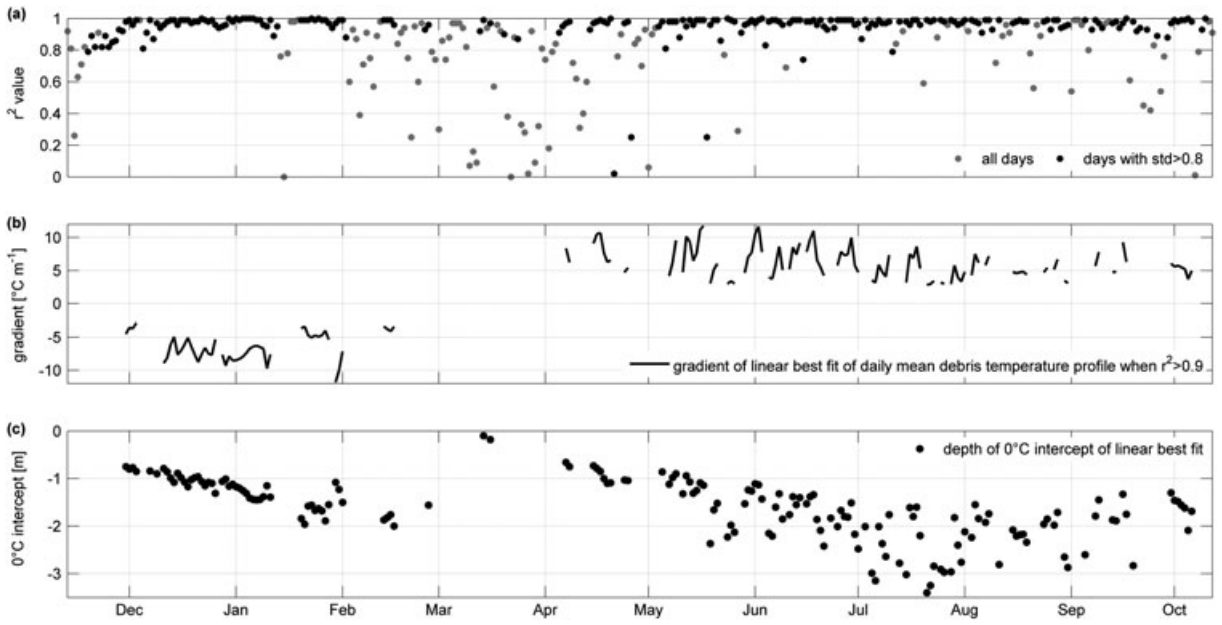

Figure 6. (a) The r^2 values of linear profiles, point highlighted in black are those for which standard deviation across all six temperature records is 0·8; (b) linear temperature gradients for days in which the r^2 value of the linear best fit exceeds 0·95; (c) the depth at which linear regression with $r^2 > 0{\cdot}95$ intercepts the 0°C isotherm.

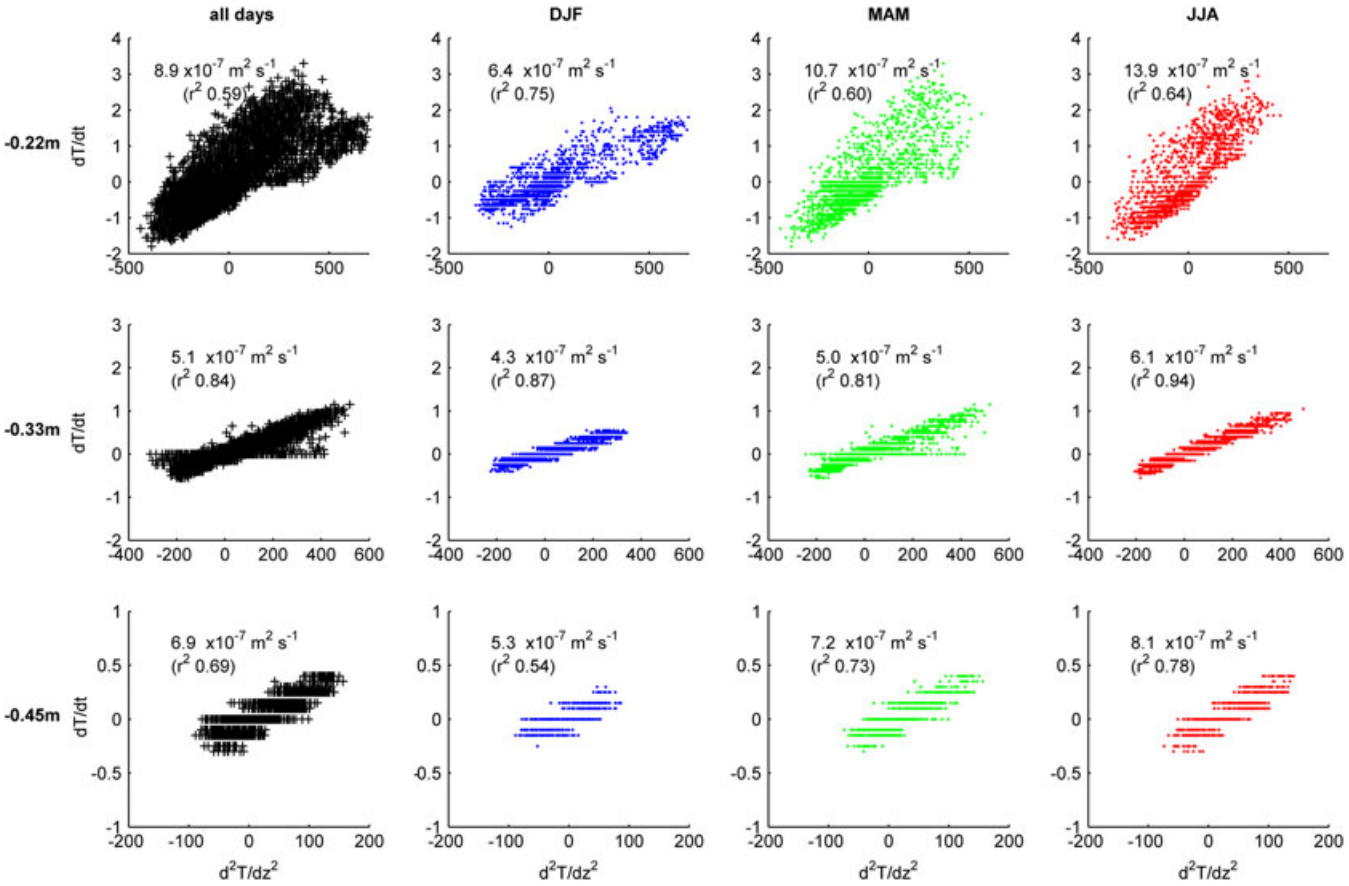

Figure 7. Scatter plots of the first derivative of hourly temperature with time against the second derivative of hourly temperature with depth at −0·22 m, –0·33 m and −0·45 m for, from left to right, all available data; DJF; MAM and JJA. This figure is available in colour online at wileyonlinelibrary.com/journal/espl

monthly mean linear temperature profiles of July, August and September all converge on a depth of ~2·5 m, which is possible in the context of local debris thickness measurements (Nicholson, 2005). The winter maximum depth and summer minimum depth of the 0°C intercept reflect the annual temperature wave penetration depth of 1·6 m determined from Figure 3, and closer inspection indicates that the deeper 0°C intercepts are nearly always associated with near-surface cooling.

Thermal Properties of the Typical supraglacial Diamict over 11 Months

Effective thermal diffusivity

The thermistors used in this study are not sufficiently precise to capture the small temperature changes occurring at 0·65 m, so effective thermal diffusivities are presented for only the thermistors at 0·22, 0·33 and 0·45 m. Scatter plots of the derivatives (Figure 7) show how the limited precision of the thermistors affects the data at depth. The scatter around the line of best fit is larger at 0·22 m than at greater depths in the debris. The ·scatter at 0·22 and 0·33 m is greater in spring than in other seasons and phase changes at 0·33 m are clearly evident in the cluster of points that show no change in temperature with time. The value of κ_e exhibits a minimum at 0·33 m and is lower in winter than summer at all levels.

Transient changes in daily κ_e, computed as the gradient of the daily linear best fit (Figure 8), show significant variation over the 11 month period, but are relatively stable within the main ablation season. Large spikes in κ_e at the beginning of February are likely to be associated with the melting of the snowcover, following a three day period of high air temperatures (Figure 5), but this effect is confined to the upper layers. A portion of the seasonal variation in κ_e can be attributed to the temperature-dependency of κ_e but the largest variation occurs when mean daily temperature is ~0°C indicating that phase changes and the role of liquid water exert a strong influence on the computed κ_e (Figure 9). Average κ_e through 0·22–0·45 m in summer (JJA) is $9{\cdot}50 \pm 0{\cdot}09 \times 10^{-7}\ m^2\ s^{-1}$, and for the stable period in winter from 15 December–5 January is $6{\cdot}98 \pm 0{\cdot}12 \times 10^{-7}\ m^2\ s^{-1}$.

Effective thermal conductivity

Assuming a 10% error on the bulk volumetric heat capacity, and that the debris is dry, the bulk summer (JJA) k_e for dry debris is $1{\cdot}29 \pm 0{\cdot}13\ W\ m^{-1}\ K^{-1}$ and for winter is $0{\cdot}95 \pm 0{\cdot}10\ W\ m^{-1}\ K^{-1}$. The 10% uncertainty on the bulk volumetric heat capacity accounts for the fact that the properties of the debris solid are not well known. For example, the specific heat capacity for granite (~$790\ J\ kg^{-1}\ K^{-1}$), would give k_e values for dry granitic debris of $1{\cdot}36 \pm 0{\cdot}14\ W\ m^{-1}\ K^{-1}$ and $1{\cdot}00 \pm 0{\cdot}10\ W\ m^{-1}\ K^{-1}$ for summer and winter, respectively. Other lithologies, such as limestones have even higher specific heat capacities, and choosing the properties of a completely inappropriate lithology such a dolomite for this site would result in differences in k_e greater than the stated error. If the voids in the debris are ice- or water-filled the bulk volumetric heat capacity increases by 50 and 100%, respectively, for the given porosity of 0·33, with correspondingly large impacts on the computed k_e. It is more likely that the debris layer is not fully saturated and the computed k_e for summer (liquid water) and winter (solid ice) if 10% (20%) of the void fraction fill of air is replaced with water is $1{\cdot}42 \pm 0{\cdot}14$ ($1{\cdot}55 \pm 0{\cdot}15$) and $0{\cdot}99 \pm 0{\cdot}09$ ($1{\cdot}04 \pm 0{\cdot}10$) $W\ m^{-1}\ K^{-1}$, respectively.

Sensitivity analysis has shown that modelled sub-debris ablation rates respond linearly to variation in the effective thermal conductivity (Nicholson, 2005; Reid and Brock, 2010). Depth-averaged estimates of k_e from measured ablation rate and surface and ice temperatures (Brock *et al.*, 2010) cannot reveal anything about the vertical structure of thermal conductivity. At our study site the vertical variation in κ_e and k_e is not monotonic with depth, even over the depth penetrated by the diurnal cycle, as might be expected if the variation was strictly a function of the temperature variation with depth. This indicates that the depth variation of k_e cannot be fully predicted from a sub-debris temperature field alone.

Observations of Surface Albedo

Measured albedo near the sites ranged from $< 0{\cdot}1$ to $> 0{\cdot}9$. The mean measured value was 0·3, but with 62% of the measurements falling between 0·1 and 0·3, the median value of 0·2 is more representative of the typical surface reflectance of the surface in dry conditions. This is higher than the albedo

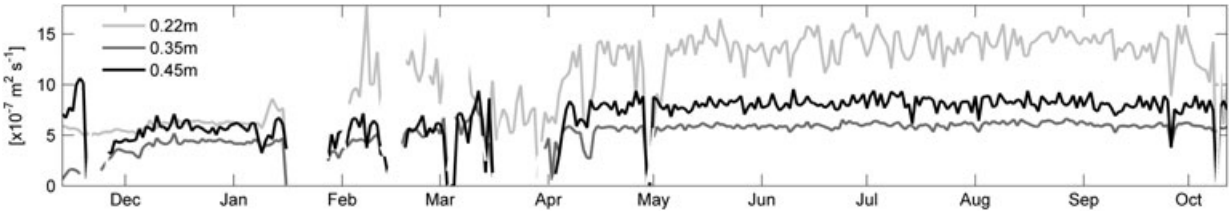

Figure 8. Daily effective diffusivity at −0·22 m, –0·33 m and −0·45 m. Times with snowcover or when non-conductive processes are influential, have been removed by removing times where the daily temperature range is below one standard deviation of the mean for that depth.

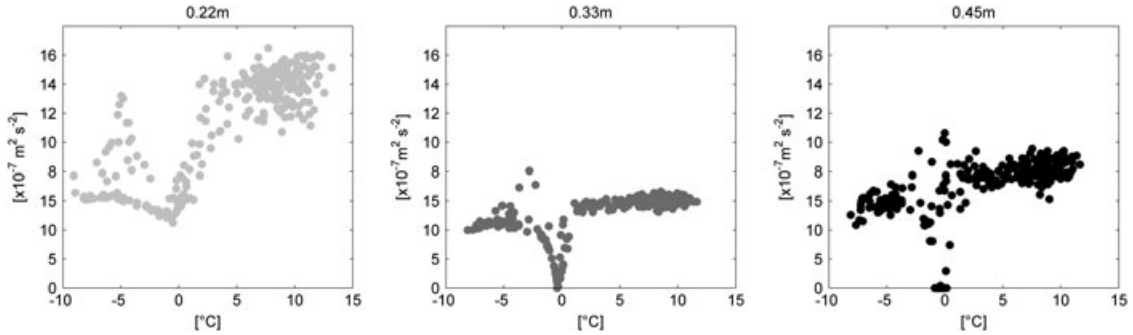

Figure 9. Dependence of derived effective diffusivity on daily mean temperature over the whole sample period excluding the sections excluded from Figure 8.

measured on nearby sloping ice faces (<0·1) that were covered in moist dust deposited from the debris section above. Overhanging ice cliffs and forays into ice caves show that glacier ice is typically much cleaner than exposed and melting ice faces that are covered in deposited dust. In general, wetting the surface of the debris lowers the albedo (Nicholson, 2005), but measurements of wetted debris were not made at this site; the measurements on the dirty ice faces provide a lower bound.

Observations of Debris Thickness

Measurements around the thermistor sites show that local debris thickness varies between 0·5 and 2·0 m within an area of few tens of square metres, which is both a cause and result of the uneven surface topography. The melt-out of debris-filled crevasses can create localized deposits with a debris cover of 3 to 4 m in thickness in excess of 3 m in thickness. Topographic highs have the thickest debris cover while thinner debris cover exists on the slopes. Collapse of ice faces, slumping and screefall down slopes gradually redistributes the debris over time resulting in slow temporal changes in debris thickness.

In the upper debris-covered portion of the glacier the distribution of debris thickness is positively skewed, and down-glacier the distribution becomes more normally distributed as the debris cover thickens (Figure 10). These data indicate that the debris thickness at a given distance from the terminus is better represented in terms of a probability distribution than a single value, and that the appropriate distribution varies with the maturity of the debris cover.

Discussion and Conclusions

On the basis of data presented here, a number of conclusions can be made about the properties and processes operating within the supraglacial debris cover on Ngozumpa glacier. Of particular interest is (i) how they affect the manner in which debris properties can be measured to determine model inputs and (ii) the ways in which they may influence spatially distributed modelling of debris-covered glaciers over multi-annual timescales. Key properties of the debris layer are the effective thermal conductivity, the surface albedo and the debris thickness. Observations and model results indicate that melting beneath debris less than ~0·5 m thick is most sensitive to debris thickness (Nicholson, 2005).

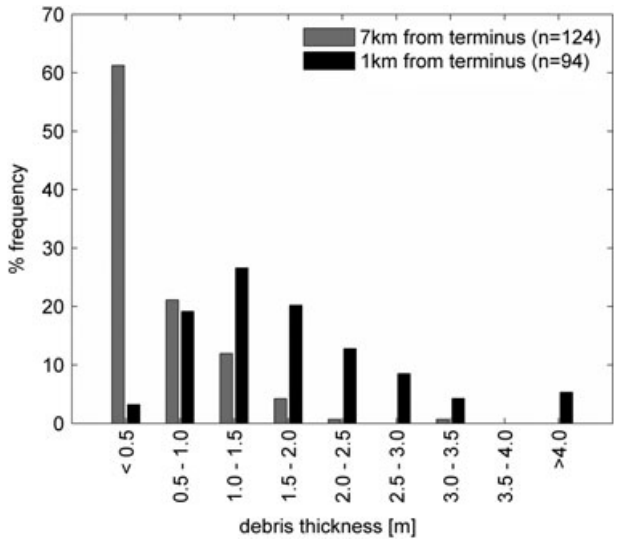

Figure 10. Sampled debris thickness distribution at 1 and 7 km from the glacier terminus (see Figure 1) shows the debris gets thicker towards the terminus and also the distribution of the debris thickness becomes less skewed.

Hinkel (1997) noted that it is not possible to verify field-determined thermal properties of soils without laboratory measurements, and that estimates of effective thermal diffusivity are especially problematic because values vary through time and space. Our field data provide information on the nature of the thermal properties of the debris in its supraglacial location.

Determining values for thermal conductivity by the method used here requires a period of stable meteorological conditions over successive days. Further, to obtain estimates of κ_e that are not significantly affected by phase changes only data from the dry conditions within an established thermal season should be used. Our work shows the limitations imposed on the method by thermistors that are not sufficiently high precision, and a minimum precision of 0·01°C would be better (Zhang and Osterkamp, 1995), and may have allowed thermal diffusivity to be computed at greater depth in the profile where temperature variations were smaller.

The calculated κ_e is higher in summer than in winter at all depths in the debris layer. This change is not progressive but rather it changes when the debris temperature changes through 0°C. This shift results from the different thermal conductivity of frozen and liquid water, in addition to the slight temperature dependency of thermal conductivity of all media on ambient temperature. Our results indicate that, if the glacier is to be modelled over annual cycles, κ_e should be calculated at both the thermal maximum and minimum or, if this is not possible, adjustment to the thermal properties of the debris should be made to account for seasonality to enable accurate modelling of the onset and ending of the ablation season.

In the absence of knowledge on the stratigraphy of a debris layer, bulk thermal and compositional properties are usually applied over the whole depth of the debris cover. Although the variation in κ_e shows a shift above and below the 0°C temperature threshold, variation with depth at this site is not monotonic, indicating that these variations with depth are not only a product of ambient temperature, but also the specific stratigraphy of the debris layer. This will be difficult to account for in any model as for most debris-covered glaciers, reworking of surface debris is likely to result in non-uniform stratigraphy.

Determining k_e from κ_e requires knowledge of the lithology because bulk volumetric heat capacity varies considerably for different lithologies. The void fill of the debris layer also has a large influence on the computed k_e. Field observations indicate that while supraglacial debris can be expected to contain some moisture it is generally well-drained through most of the depth, but can have a water-rich zone at the ice interface. Although the geometrical mean porosity of sand and blocky material may be similar it can be observed in the field that sand will retain more moisture than the blocky material which would result in a higher overall thermal conductivity during times when liquid water is retained in the finer material. The moisture-content of the debris cover is generally unknown and it is not clear if model accuracy would be significantly improved by the explicit inclusion of moisture migration within the debris layers, but observations of a representative thickness of the wetted layer at the interface would provide supplementary information for model set up and moisture content stratification could be a useful modification of depth-averaged k_e values.

Surface albedo is predominantly controlled by lithology; for example on the neighbouring Khumbu glacier a longitudinal band of darker schistic material can be seen (Fushimi *et al.*,

1980; Casey *et al.*, 2012), but even with more uniform lithology as found on the Ngozumpa glacier, surface albedo can vary significantly on a mature debris cover. It remains to be seen if this spatial variability is sufficient to play a role in the development of ablation topography on the glacier or if that process is governed primarily by debris thickness variations. Measurements of both wet and dry surface albedo should be made in order constrain this property for different surface conditions.

Debris thickness increases down-glacier within the debris-covered zone. However, the down-glacier trend in mean debris thickness is a poor predictor of debris thickness at a single point as the debris thickness varies widely over small spatial scales. For distributed glacier modelling the debris thickness distribution is better represented as a probability density function. On the Ngozumpa glacier this probability density function evolves from a skewed distribution to a more normal distribution down-glacier as the mean thickness increases, but the applicability of such a spatial variation in debris thickness distribution to other glaciers requires assessment with field measurements. Determining debris thickness from a linear extrapolation of the mean temperature profiles can produce misleading results if meteorological conditions are fluctuating from day to day.

Concerning the role of non-conductive heat transfer processes, the data from the Ngozumpa glacier indicate that conductive processes dominate in matrix-supported debris layers in summer, but coarser debris, or coarse surface layers overlying a matrix-supported debris layer are likely to experience heat transfer by ventilation throughout the depth of the coarse layer, and phase changes are evident in the spring and fall seasons and associated with snowfall events. Phase changes within the debris cover associated with seasonal changes are important for defining the seasonal duration of sub-debris melt and resultant total annual ablation. This means it is important to be able to model the thermal dynamics of the debris layer in the shoulder seasons to define the sub-debris ablation season. It would also be valuable to make concurrent measurements within different debris lithologies and grain sizes so that the impact of differences in the debris can be separated from the differences in meteorological conditions. Observations of permafrost sites have shown that coarse surface layers result in a cooler sub-surface temperature field (e.g. Harris and Pedersen, 1998; Hanson and Hoelzle, 2005; Juliussen and Humlum, 2008) compared to either rock or matrix supported sediments and this has been used to preserve infrastructure in frozen ground (e.g. Cheng *et al.*, 2008, and references cited therein). Cool temperature anomalies beneath blocky material are commonly attributed to thermally-driven convection in winter, which efficiently exchanges warmer air from the debris voids for cooler air from the surface, and stable stratification of air in the void spaces of the blocky layer in summer. However, many processes can contribute to the temperature anomaly (Juliussen and Humlum, 2008), and the relative importance of different processes has not been resolved. For example, the thermal anomaly associated with coarse debris can be equally well modelled as a result of the lower effective thermal conductivity layer of a low porosity blocky layer, without recourse to ventilation processes (Gruber and Hoelzle, 2008) and the roughness of the blocky surface can make it form more effective heat bridges through snowcover to atmospheric temperature variations (Juliussen and Humlum, 2008). The association of coarse surface material with cool sub-surface temperature anomalies (Harris and Pedersen, 1998; Cheng *et al.*, 2008) suggests that the spatial distribution of blocky material at the surface of the debris layer can be expected to exert an influence on the sub-debris ice melt.

If ice is taken to be at the melting point (e.g. Nakawo and Young, 1982; Nicholson and Benn, 2006; Reid and Brock, 2010), model results are only applicable within the established melt season on mid- to low-latitude glaciers, that can be assumed to be temperate. Application of sub-debris ablation models over longer timescales, or colder environments, requires inclusion of the en-glacial heat flux.

Application of simplified energy balance models using diurnal linear representations of vertical temperature gradients through the debris is appropriate only in unstratified debris layers during periods with stable meteorological conditions within established winter or summer seasons. However, averaged over longer time intervals, errors in computed ablation rate may tend to cancel out.

Assessing the impact of (i) the ice temperature field, (ii) incorporation of phase changes and (iii) the timescale for determining temperature gradients to drive heat flux would be a useful next step in determining the best approaches for mass balance modelling of debris-covered glaciers over a range of temporal and spatial scales, in addition to a quantitative assessment of the sensitivity of models of various complexity to both the debris and meteorological input parameters. More empirical data from debris-covered glaciers is required both to aid our understanding of ablation at the surface of these glaciers and to validate modelling efforts.

Acknowledgements—Fieldwork was funded by a Quaternary Research Association New Workers Award, the Royal Scottish Geographical Society, the American Alpine Club and the School of Geography and Geosciences, St Andrews University. The authors wish to thank Kat Hands and Richard Bates for their assistance and good company in the field, and acknowledge the hospitality and support of the Sharmas and their staff at the Gokyo Resort in Nepal. Thanks also to two anonymous reviewers who provided very constructive reviews that greatly improved the clarity of the final paper.

References

Benn DI, Evans DJA. 2010. *Glaciers and Glaciation*, 2nd edn. Hodder Education: London.

Benn DI, Owen LA. 2002. Himalayan glacial sedimentary environments: a framework for reconstructing and dating the former extent of glaciers in high mountains. *Quaternary International* **97–98**: 3–25.

Benn DI, Bolch T, Dennis K, Gulley J, Luckman A, Nicholson LI, Quincey D, Thompson S, Toumi R, Wiseman S. 2012. Response of debris-covered glaciers in the Mount Everest region to recent warming, and implications for outburst flood hazards. *Earth-Science Reviews* **114**: 156–174.

Benn DI, Wiseman S, Hands KA. 2001. Growth and drainage of supraglacial lakes on debris mantled Ngozumpa Glacier, Khumbu Himal, Nepal. *Journal of Glaciology* **47**(159): 626–638.

Brock BW, Mihalcea C, Kirkbride MP, Diolaiuti G, Cutler MEJ, Smiraglia C. 2010. Meteorology and surface energy fluxes in the 2005–2007 ablation seasons at the Miage debris-covered glacier, Mont Blanc Massif, Italian Alps. *Journal of Geophysical Research-Atmospheres* **115**: D09106. DOI: 10.1029/2009jd013224

Casey KA, Kääb A, Benn DI. 2012. Geochemical characterization of supraglacial debris via *in situ* and optical remote sensing methods: a case study in Khumbu Himalaya, Nepal. *The Cryosphere* **6**: 85–100.

Cheng G, Sun Z, Niu F. 2008. Application of the roadbed cooling approach in Qinghai-Tibet railway engineering. *Cold Regions Science and Technology* **53**(3): 241–258.

Conway H, Rasmussen LA. 2000. Summer temperature profiles within supraglacial debris on Khumbu Glacier, Nepal. In *Debris-covered Glaciers*, Nakawo M, Raymond CF, Fountain A (eds), IAHS-AISH Publication 264. IAHS Press: Wallingford; 89–97.

Drewry DJ. 1972. A quantitative assessment of dirt-cone dynamics. *Journal of Glaciology* **11**(63): 431–446.

Farouki OT. 1981. *Thermal Properties of Soils*, CRREL Monograph 81–1. United States Army Corps of Engineers, Cold Regions Research and Engineering Laboratory: Hanover, NH.

Fujii Y. 1977. Field experiment on glacier ablation under a layer of debris cover. *Seppyo Journal of the Japanese Society of Snow and Ice* **39**: 20–21.

Gruber S, Hoelzle M. 2008. The cooling effect of coarse blocks revisited: a modelling study of a purely conductive mechanism. In *Proceedings, 9th International Conference on Permafrost*, Kane DL, Hinkel KM (eds). Institute of Northern Engineering, University of Alaska: Fairbanks, Alaska; 557–561.

Han HD, Ding YJ, Liu SY. 2006. A simple model to estimate ice ablation under a thick debris layer. *Journal of Glaciology* **52**(179): 528–536.

Hands KA. 2004. Evolution of Supraglacial Lakes on Ngozumpa Glacier, Nepal. Unpublished PhD Thesis, University of St Andrews.

Hanson S, Hoelzle M. 2005. Installation of a shallow borehole network and monitoring of the ground thermal regime of a high alpine discontinuous permafrost environment, eastern Swiss Alps. *Norsk Geografisk Tidsskrift – Norwegian Journal of Geography* **59**(2): 84–93.

Harris SA, Pedersen DE. 1998. Thermal regimes beneath coarse blocky debris. *Permafrost and Periglacial Processes* **9**: 107–120.

Hinkel KM. 1997. Estimating seasonal values of thermal diffusivity in thawed and frozen soils using temperature time series. *Cold Regions Science and Technology* **26**(1): 1–15.

Humlum O. 1997. Active layer thermal regime at three rock glaciers in Greenland. *Permafrost and Periglacial Processes* **8**: 187–254.

Jansson P, Fredin O. 2002. Ice sheet growth under dirty conditions: implications of debris cover for early glaciation advances. *Quaternary International* **95–96**: 35–42.

Juliussen H, Humlum O. 2008. Thermal regime of openwork block fields on the mountains Elgahogna and Solen, Central-eastern Norway. *Permafrost and Periglacial Processes* **19**: 1–18.

Kostlin EC, Molyneux TG. 1992. The geology of the higher Himalayas of the Solo-Khumbu region of eastern Nepal. *Geobulletin* **35**(2): 3–7.

Loomis SR. 1970. Morphology and ablation processes on glacier ice. *Proceedings of the Association of American Geographers* **12**: 88–92.

Mattson LE, Gardner JS, Young GJ. 1993. Ablation on debris covered glaciers: an example from the Rakhiot Glacier, Punjab, Himalaya. In *Snow and Glacier Hydrology*, Young GJ (ed.), IAHS-IASH Publication 218. IAHS Press: Wallingford; 289–296.

Nakawo M, Young GJ. 1981. Field experiments to determine the effect of a debris layer on ablation of glacier ice. *Annals of Glaciology* **2**: 85–91.

Nakawo M, Young GJ. 1982. Estimate of glacier ablation under a debris layer from surface temperature and meteorological variables. *Journal of Glaciology* **28**(98): 29–34.

Nicholson LI. 2005. Modelling Melt Beneath Supraglacial Debris: Implications for the Climatic Response of Debris-covered Glaciers. Unpublished PhD Thesis, University of St Andrews.

Nicholson LI, Benn DI. 2006. Calculating ice melt beneath a debris layer using meteorological data. *Journal of Glaciology* **52**(178): 463–470.

Østrem G. 1959. Ice melting under a thin layer of moraine, and the existence of ice cores in moraine ridges. *Geografiska Annaler* **51**(4): 228–230.

Putkonen J. 1998. Soil thermal properties and heat transfer processes near Ny-Ålesund, northwestern Spitsbergen, Svalbard. *Polar Research* **17**(2): 165–179.

Quincey DJ, Luckman A, Benn DI. 2009. Quantification of Everest-region glacier velocities between 1992 and 2002, using satellite radar interferometry and feature tracking. *Journal of Glaciology* **55**(192): 596–606.

Reid TD, Brock BW. 2010. An energy-balance model for debris-covered glaciers including heat conduction through the debris layer. *Journal of Glaciology* **56**(199): 903–916.

Reznichenko N, Davies T, Shulmeister J, McSaveney M. 2010. Effects of debris on ice-surface melting rates: an experimental study. *Journal of Glaciology* **56**(197): 384–394.

Sakai A, Fujita K. 2004. Evaporation and percolation effect on melting at debris-covered Lirung Glacier, Nepal Himalayas, 1996. *Bulletin of Glaciological Research* **21**: 9–15.

Sakai A, Takeuchi N, Fujita K, Nakawo M. 2000. Role of supraglacial ponds in the ablation process of a debris-covered glacier in the Nepal Himalayas. In *Debris-covered Glaciers*, Nakawo M, Raymond CF, Fountain A (eds), IAHS-AISH Publication 264. IAHS Press: Wallingford; 119–132.

Scherler M, Hauck C, Hoelzle M, Stähli M, Völksch I. 2010. Meltwater infiltration into the frozen active layer at an alpine permafrost site. *Permafrost and Periglacial Processes* **21**(4): 325–334.

Singh P, Kumar N, Ramasastri KS, Singh Y. 2000. Influence of a fine debris layer on the melting of snow and ice on a Himalayan glacier. In *Debris-covered Glaciers*, Nakawo M, Raymond CF, Fountain A (eds), IAHS-AISH Publication 264. IAHS Press: Wallingford; 63–69.

Vondermuhll D, Haeberli W. 1990. Thermal-characteristics of the permafrost within an active rock glacier Murtel Corvatsch, Grisons, Swiss Alps. *Journal of Glaciology* **36**(123): 151–158.

Williams PJ, Smith MW. 1989. *The Frozen Earth: Fundamentals of Geocryology. Studies in Polar Research*. Cambridge University Press: Cambridge; 306.

Zhang T, Osterkamp TE. 1995. Considerations in determining thermal diffusivity from temperature time series using finite difference methods. *Cold Regions Science and Technology* **23**: 333–341.